Characterization and Modeling of a Microfluidic Dielectrophoresis Filter for Biological Species

Haibo Li, Yanan Zheng, Demir Akin, and Rashid Bashir, *Senior Member, IEEE*

***Abstract*—Microfabricated interdigitated electrode array is a convenient form of electrode geometry for dielectrophoretic trapping of particles and biological entities such as cells and bacteria within microfluidic biochips. We present experimental results and finite element modeling of the holding forces for both positive and negative dielectrophoretic traps on microfabricated interdigitated electrodes within a microfluidic biochip fabricated in silicon with a 12-μm-deep chamber. Anodic bonding was used to close the channels with a glass cover. An Experimental protocol was then used to measure the voltages necessary to capture different particles (polystyrene beads, yeast cells, spores and bacteria) against destabilizing fluid flows at a given frequency. The experimental results and those from modeling are found to be in close agreement, validating our ability to model the dielectrophoretic filter for bacteria, spores, yeast cells, and polystyrene beads. This knowledge can be very useful in designing and operating a dielectrophoretic barrier or filter to sort and select particles entering the microfluidic devices for further analysis. [1181]**

***Index Terms*—Dielectrophoretic filter, interdigitated electrode, microfluidic biochip.**

I. Introduction

DIELECTROPHORESIS (DEP) is the movement of a particle in a nonuniform ac electrical field. It occurs through the interaction of the induced electrical polarization charge with the nonuniform electric field and can induce movement of the particle toward either the location with the greatest gradient in the electric field strength (∇E^2) (positive DEP), or location with smallest electric field gradient (negative DEP), depending on the dielectric constant of the particle relative to that of the medium [1]. DEP-based techniques have been successfully used for many biological applications to date, such as separations of viable and nonviable yeast cells [2], [3], separation of live and heat-treated listeria bacteria [4], isolation and detection of sparse cancer cells, concentration of cells from dilute suspensions, and trapping and positioning of individual cells for characterization [5]. Among these, the simplest method of practical dielectrophoretic separation is that of flow separation [6]. By this method, the mixture of particles to be separated is pushed by an external source, such as a syringe or peristaltic pump, through an enclosed separation chamber with an electrode array on the bottom. There is a single inlet and outlet port. The separation strategy is like this: when two populations of particles are pumped across the electrode array, particles of one population experience positive dielectrophoresis and are trapped at the electrode edges, whilst the other experiences negative dielectrophoresis and is pushed by the flow through the outlet, where the particles can be collected. After the latter particles have left the chamber, the electric field is removed and the former particles are released and pumped to the outlet where they can be collected in another container. In addition, it has been found that particles of many populations, all of which exhibited negative dielectrophoresis, could be separated by means of an original combination of dielectrophoretic and gravitational field flow fractionation [7]–[9]. In this method, negative DEP forces levitate particles to equilibrium positions in a flow-velocity profile, particles at different heights in the flow stream move at different velocities and can be fractionate based on their different retention times in the chamber. Most studies of biological suspensions used a flat, transparent horizontal microchannel that was formed by a spacer ($\sim 400\ \mu$m height is normally used) sandwiched between the bottom electrode plate and a top glass plate. It is known that the magnitude of DEP force reduces quickly with distance above the electrodes, and as a consequence the particles will experience appreciable dielectrophoretic forces only in the area near the electrodes [10]. Thus the devices with large chamber height are not suitable for DEP trapping, since not only the particles experiencing negative DEP cannot be stopped, some particles experiencing positive DEP have to pass over the electrodes at distance too large for the dielectrophoretic force to be sufficient to trap them.

In this study, we built up a dielectrophoretic filter with a thin ($\sim\ 12\ \mu$m) microchannel etched into single-crystalline silicon (SCS) substrate, which can trap particles exhibiting either positive or negative DEP. We compared experimental results on the capturing capability of an interdigitated electrode array, with predictions from a specifically developed simulation environment. This environment was developed using Finite Element and numerical methods to obtain near-electrode-plane high-order DEP forces and other forces on particles in the fluidic flow in both horizontal and vertical directions. We can thus characterize our thin DEP filter for both negative and positive traps on interdigitated electrodes and understand the operation of the device as a particle filter and separator. We first used polystyrene beads to validate our ability to model the force field in

Manuscript received October 16, 2003; revised June 1, 2004. This work was supported through a cooperative agreement with the Agricultural Research Service of the United States Department of Agriculture, project number 1935-42000-035. Subject Editor D. J. Beebe.

H. Li and D. Akin are with the School of Electrical and Computer Engineering, Purdue University, West Lafayette, IN 47907-1285 USA.

Y. Zheng is with the Department of Biomedical Engineering, Purdue University, West Lafayette, IN 47907-1285 USA.

R. Bashir is with the School of Electrical and Computer Engineering, Purdue University, West Lafayette, IN 47907-1285 USA and also with the Department of Biomedical Engineering, Purdue University, West Lafayette, IN 47907-1285 USA (bashir@ecn.purdue.edu).

Digital Object Identifier 10.1109/JMEMS.2004.839124

the DEP filter because of their uniform and well-known dielectric properties, which eases our comparison with the modeling. Then we used different biological particles such as yeast cells, spores, and bacteria for further validation. The experimental results and those from modeling are found to be in close agreement, indicating our success in the analysis of force field in our modeling environment, including multi-order DEP forces, hydrodynamic drag and lifting forces, and sedimentation force. It also allows us to accurately determine the sub-pico-Newton forces at the microscale, once we know the position of the particle in the chamber. This knowledge can be very useful in designing and operating a dielectrophoretic barrier or filter to sort and select particles entering the microfluidic devices for further analysis.

II. Theoretical Background

Particles in the dielectrophoretic filter experience forces from dielectrophoresis, gravity, hydrodynamic drag, and lifting effects. These are briefly described below.

A. Dielectrophoretic Forces Over Interdigitated Electrodes

The time-averaged dielectrophoretic force F for a dielectric sphere immersed in a medium in constant field phases in space is given by [4] and valid for all particles in the effective-moment approximation

$$F = 2\pi\varepsilon_0\varepsilon_m r^3 \mathrm{Re}[f_{\mathrm{CM}}]\nabla|E_{\mathrm{rms}}|^2 \tag{1}$$

where ε_0 is the vacuum dielectric constant, r is the particle radius, E_{rms} is the root mean square value of the electric field, and f_{CM} is well known as the Clausius–Mossotti factor [4]

$$f_{\mathrm{CM}} = \frac{\varepsilon_p^* - \varepsilon_m^*}{\varepsilon_p^* + 2\varepsilon_m^*} \tag{2}$$

where ε_p^* and ε_m^* are the relative complex permittivities of the particle and the medium respectively and are each given by $\varepsilon^* = \varepsilon + \sigma/(j\omega)$, where ε is the permittivity and σ is the conductivity of the particle or medium, and j is $\sqrt{-1}$.

Formula (1) was derived by the interaction of a nonuniform electric field with dipole moment induced in the particle and is applicable in the cases where the particle is much smaller than the electric field nonuniformities. This first-order approximation is not sufficiently accurate when the small particle is close to the electrode edges or at field nulls, higher order moments have to be accounted by the formula given by Washizu and Jones [11], [12]:

$$\vec{F}_{\mathrm{total}} = \sum_0^\infty \vec{F}_n = \sum_0^\infty -\nabla U_n \tag{3}$$

where n refers to the force order, and

$$U_n = -\frac{2\pi\varepsilon_m K_n r^{(2n+1)}}{(2n+1)!!} \sum_{i+j+k=n} \frac{1}{i!j!k!} \left[\frac{\partial^n \Phi}{\partial x^i \partial y^j \partial z^k}\right]^2 \tag{4}$$

where Φ is the electrostatic potential of the external electric field, K_n is the nth-order Clausius–Mossotti factor

$$K_n = \frac{n(2n+1)(\varepsilon_p - \varepsilon_m)}{n\varepsilon_p + (n+1)\varepsilon_m}. \tag{5}$$

Parallel interdigitated electrode array is a convenient form of electrode geometry for dielectrophoretic trapping of particles. Although the geometry is simple, neither the electric potential nor the field has an exact analytical expression. Prior work has been reported on the analyzes of the electric potential or field and DEP forces over the interdigitated electrodes. Gerwen *et al.* [13] derived an analytical approximation solution of the electric potential by using Schwarz-Christoffel conformal transformation. Wang *et al.* [14] calculated the electric field using Green's theorem and Clague *et al.* [15] obtained an analytic approximation solution for the gradient in the electric field strength (∇E^2) by using a different Green's function. Morgan *et al.* [16] presented dielectrophoretic forces in infinite Fourier series. All these series expansion solutions are approximations to a geometry for which an analytical representation has not been determined. Numerical solutions were also studied for the first-order DEP forces by Green *et al.* using finite element method [17]. Recently, Voldman *et al.* [18], [19] used commercially available finite element program to derive electric field data and then calculated the DEP forces to any higher order moments, though applying to planar and extruded quadrupole traps, giving an approach to obtain the DEP forces in a simple step.

B. Hydrodynamic Drag Force

The hydrodynamic drag force on a particle of radius r is dependent on the velocity of the particle relative to that of the fluid medium. The horizontal drag force on a particle in contact with a wall is given by the modified Stokes equation [20]

$$F_{\mathrm{HD-drag}} = 6\pi k r \eta \upsilon_m \tag{6}$$

where η is the dynamic viscosity of the fluid, υ_{m} is the velocity of the medium fluid at the center of the particle, k ($k > 1$, for particle in contact with the wall, $k \approx 1.7$) is a nondimensional factor accounting for the wall effects. The fluid is usually assumed to follow a parabolic laminar flow profile such that υ at a distance x from the bottom of the chamber is

$$\upsilon = 6\langle\upsilon\rangle \frac{x}{h}\left(1 - \frac{x}{h}\right) \tag{7}$$

where $\langle\upsilon\rangle$ is the mean velocity of the flow and h is the top to bottom spacing of the chamber walls

$$\langle\upsilon\rangle = \frac{V}{wh} \tag{8}$$

where w is the width and wh is the cross-section area of the chamber, V is the nominal flow rate in $\mu\mathrm{l/min}$. The good agreement between modeling and experimental results validates this shear flow approximation even when the particle diameter ($\sim$

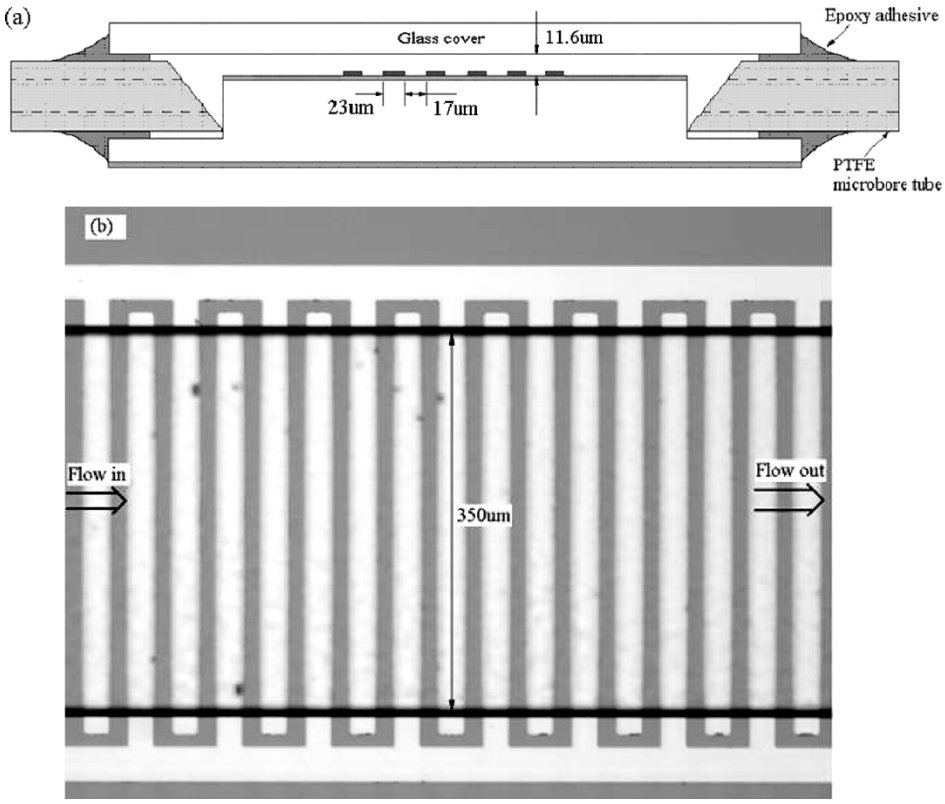

Fig. 1. Schematic plot of the device cross section in (a) and a photograph of the chamber (top view) in (b). The width of the electrodes and the spacing between two adjacent electrodes are 23 and 17 μm, respectively, and the chamber depth is 11.6 μm measured by a profilometer.

$5.4\ \mu\mathrm{m}$) occupies a significant fraction of the chamber height ($\sim 11.6\ \mu\mathrm{m}$).

C. Sedimentation Force

The sedimentation force is given by

$$F_{sedi} = \frac{4}{3}\pi r^3(\rho_p - \rho_m)g$$

where r is the radius of the particle, ρ_p, and ρ_m refer to the densities of the particle and medium respectively, and g is the gravitational acceleration constant.

D. Hydrodynamic Lifting Force

The lift force experienced by a nondeformable particle located at a small distance $x - r$ above the chamber wall is given by

$$F_{\text{lift}} \approx 0.153 r^3 \eta \frac{1}{(x-r)} \cdot \left.\frac{dv_m}{dx}\right|_{x=0}.$$

This formula was empirically derived by Williams *et al.* [21] but the nature of the lift force still remains in question. Although it is believed that this hydrodynamic lift force plays little or no role in typical DEP-Gravitational Field-Flow process [7] and our calculation shows that the maximum lifting force is about one magnitude lower than the peak vertical DEP force at 1 $\mathrm{V_{pp}}$), it is still incorporated into our modeling in order to get a complete view of the force field.

III. Experimental Details

A. Fabrication of the Device

The fabrication process of the dielectrophoretic filter is similar to the discussion in [22], here we will only briefly describe the most important features of the device. The DEP chamber was constructed by KOH-etching a depth of 11.6 μm (with smooth bottom surface and roughness less than 50 nm) and width of 350 μm into single crystalline silicon substrate using a silicon dioxide layer as the mask, then all the oxide was removed and the wafer was reoxidized to form a insulating layer of about 0.4 μm. A metal (Ti/Pt of 200/800 Å thick) pattern of interdigitated electrode array was formed at the bottom of the chamber using sputtering and lift-off. These electrodes are connected by metal traces to pads on the periphery of the chip where electrical contacts with a signal generator are established. A silicon dioxide layer of about 0.3 μm was deposited by plasma-enhanced chemical-vapor deposition (PECVD) to cover all the electrodes in the chamber and protect them. This thin layer of oxide has little effect on the DEP force according to our calculation. Deep trenches are etched to the two ends of the chamber by deep-reactive ion etch (DRIE) and microbore tubes were inserted into the inlet and outlet ports to inject and drain the liquids through the chamber. The top of the chamber was covered with a glass slide by anodic bonding. Fig. 1 shows the schematic plot of the experimental devices and the top view of the interdigitated microelectrodes. In the experiments, sample solutions were injected into the chamber using a syringe pump (World Precision

Instruments Inc., SP200i) and a 250-μl gas-tight luer-lock syringe (ILS250TLL, World Precision Instruments Inc.). The flow rate could be adjusted and precautions were taken to avoid air bubbles. An HP 33 120A arbitrary waveform generator was used as the ac signal source to produce sinusoidal signal with frequency specified at 1 MHz. The behaviors of the particle in the flow were viewed on a Nikon microscope with or without fluorescence filters and recorded by a charge-coupled device (CCD) digital camera (Pixera Penguin 600 CL, Pixera Corp., Los Gatos, CA).

B. Sample Preparations

Polystyrene beads, *Saccharomyces cerevisiae* yeast cells, *Bacillus cereus* spores, and *Listeria innocua* bacteria were chosen for the experiments. Polystyrene beads, with 2.4 and 5.4 μm in diameter, with a density $\sim$ 1.05 g/cm^3, and dielectric constant 2.5–2.6, were used (Spherotech, Inc., IL, USA). Yeast cells were cultured in an aqueous yeast extract medium and harvested and stored in a 4 °C refrigerator in the stationary phase after two days. The average size of the yeast cells is about 5 μm and can be seen under microscope without fluorescence staining. In the case that yeast cells were mixed with *Listeria* bacteria, both were stained with FITC dye and appear fluorescent green under the microscope. Bacterial spores are noted for their extreme degrees of resistance and dormancy. The enveloping structures of the mature, dormant spore consist of the spore coats, an inverted outer membrane, an inter-membrane cortex composed of peptidoglycan, and an inner-membrane surrounding the spore core or protoplast [23]. The *Bacillus cereus* spores used in our experiments have an average diameter approximately 1 μm and were suspended in DI water and stained with 3,3′-dihexyloxacarbocyanine iodide ($\mathrm{DiOC_6(3)}$) dye (green). The *Listeria innocua* bacteria are rod shaped with length of around 3 μm and diameter around 1 μm. The cells were cultured in BHI (Brain Heart Infusion) solution at 37 °C. They were harvested after 18 h with the concentration of $\sim 10^9$ cells/ml and stained with FITC dye. Upon injection into the chamber, all sample suspensions were centrifuged and washed with DI water for three times and then diluted to $\sim 10^{5\sim7}$ particles/ml with DI water. The conductivity of the final suspensions was measured to be 2.5 μS/cm by a conductivity meter (Cole–Parmer Instruments). The dynamic viscosity of the DI water is about 1.0×10^{-3} N $\cdot$ s/m^2.

C. Release Voltage Measurement

In the flow chamber, particles experiencing either negative or positive DEP stop at their equilibrium positions at a given flow rate, if the DEP forces are sufficiently high. If a particle was held in the equilibrium position at the end of two minutes, the particle was considered captured. The flow rate was adjusted and the corresponding voltage necessary to capture a particle was measured by first applying a large voltage to stop the particle, and then slowly decreasing the voltage and recording the value at which this particle just get released. More than six measurements were taken for each data point and an average value was calculated with the error bar. Over 20 chips were used in the experiments. Chips for beads experiments can be reused since beads don't stick to the surface. Chips for bacteria measurement were one-time usage because of the nonspecific binding of the bacteria. All chips are assumed to be exact the same since they were fabricated and cut from the same silicon wafer. Each experiment lasts two to three hours except the time for bacteria culture and staining.

D. Modeling

The modeling program used electric-field data from commercially available Finite Element program Ansys (version 5.7, ANSYS Inc. Canonsburg, PA) with grid spacing as small as 0.2 μm. The experimental parameters and Matlab (R12, The Mathworks, Natick, MA) was used, and we did not catalog the multiple derivatives of the electric field, instead we stored the derivatives when there was a need to calculate the higher order DEP forces. Since the electrodes are long compared to their width, the problem can be considered to be two-dimensional. For a given particle and flow rate, we calculated the DEP forces in horizontal and vertical directions to an arbitrary order until sufficient accuracy was obtained (the result converges with relative error less than 3%) in the sedimentation force, the hydrodynamic drag force, and lifting force everywhere in space. Then we determined the equilibrium positions of the particle in such a force field in the chamber by determining the zero-net-force points. In case that the particle experiences negative DEP and is levitated to against the top glass, and that the particle experiences positive DEP and is forced to the chamber bottom, only forces in horizontal forces are considered to determine the equilibrium position since the top glass and the chamber bottom have the supporting forces to balance the others in vertical direction. Extra forces due to particles nonspecific sticking to the surface or friction between particles and the surface can be either extraordinary strong or small, are not counted in the simulation.

IV. Results and Discussion

First of all, to get a sense of how the multipolar DEP forces are compared to those induced only by the dipole term, we calculated the horizontal and vertical DEP forces on a 2.4-μm-polystyrene bead with conductivity of 2×10^{-4} S/m in contact with the electrode plane in an aqueous medium with conductivity of 2.5×10^{-4} S/m at 1 V_{pp} and 1 MHz (All DEP forces were calculated with height corresponding to the position of particle center, same valid throughout the paper). Fig. 2(a) and (b) shows the horizontal and vertical DEP forces with increased multipolar orders ($n = 1$ corresponds dipole, $n = 2$ dipole, and quadrupole, $n = 3$ dipole, quadrupole, and octupole, and so on, the bold lines on the bottom axis represent the electrodes, same for the followed figures). It is seen that the DEP forces converge quickly at about $n = 3$ or 4. When $n = 4$, the calculated horizontal DEP force is about 20% larger than that when $n = 2$ (dipole), and the vertical DEP force increases by about 40%. This is significant for accurate prediction in our modeling. For the balance of time efficiency and accuracy in our calculation, $n = 4$ was normally made with relative error less than 3%.

Fig. 3 shows the capture of 2.4 μm polystyrene beads against the fluidic flow at around 0.05 μl/min (corresponding to a velocity of ~ 117 μm/s at the center of the bead in contact with the top or bottom of the chamber) with 20 V_{pp} applied to the

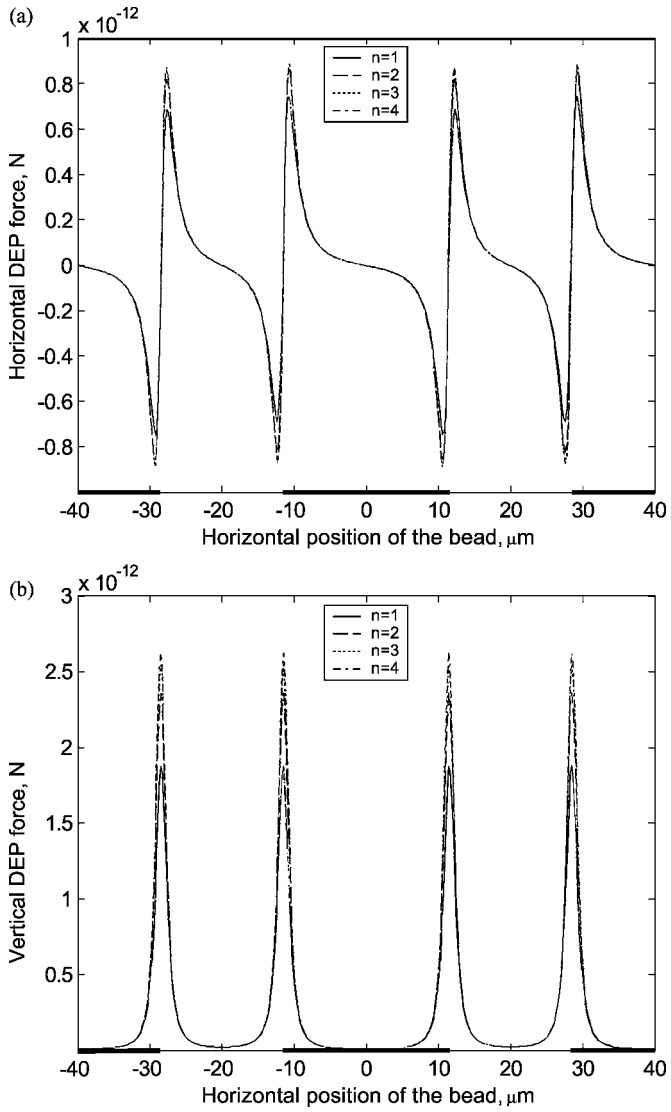

Fig. 2. Horizontal (a) and vertical (b) DEP forces on a 2.4-μm-polystyrene bead with conductivity of 2×10^{-4} S/m in contact with the electrode plane in an aqueous medium with conductivity of 2.5×10^{-4} S/m at 1 V_{pp} and 1 MHz with increased multipolar orders (n = 1 corresponds dipole, n = 2 dipole and quadrupole, n = 3 dipole, quadrupole and octupole, and so on), the bold lines on the bottom axis represent the electrodes.

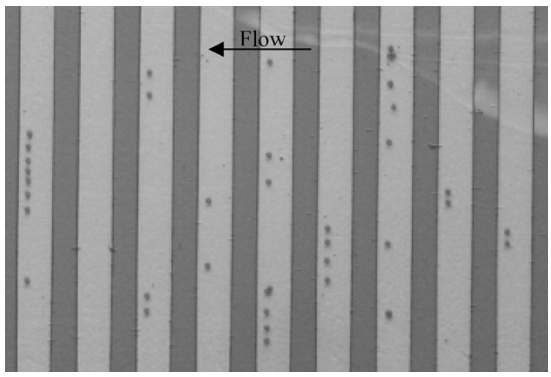

Fig. 3. Capture of 2.4-μm-polystyrene beads above the electrodes against the fluidic flow at around 0.05 μl/min with 20 V_{pp} applied to the electrodes. The beads were levitated to contact the top glass and shifted from the center of the electrode due to the hydrodynamic drag force.

electrodes. It is seen that the beads were shifted from the center of the electrode (DEP force minimum) due to the hydrodynamic drag force. Careful observation revealed that the beads were levitated to contact the top glass, instead of being in contact with the electrodes. This is quite consistent with our analysis of the forces exerted on the beads. Fig. 4(a) shows the horizontal DEP force changes with height from 1.2 μm (where beads in contact with the electrodes) to 4.2 μm by taking the conductivity of the beads to be 2×10^{-4} S/m [19], at 1 V_{pp} and 1 MHz. The calculated polarization factor is -0.473. It seems apparent at the first sight from Fig. 4(a) that the beads experiencing negative DEP should collect not only above the centers of the electrodes, but also above the centers of the intervals between any two neighboring electrodes, since the horizontal DEP force directs them to those places. This is contradictory to our experimental observation: the beads only collect above the electrodes. Further study to the horizontal DEP force revealed that the beads are directed only to the electrode centers at height above 8 μm, as shown in Fig. 4(b), the interelectrode minima disappear and the slope becomes positive to push beads away, which is consistent with our previous study of the DEP force on interdigitated electrodes [4]. Meanwhile, the vertical DEP forces at different heights are shown in Fig. 4(c) and (d). It is seen that the force maxima are above the electrode tips and a minimum is above the center of the electrode. We plot the latter along z direction (vertical) at the middle of the electrode in Fig. 4(e). The calculated force magnitude ranges from about 8×10^{-15} N to 2.4×10^{-14} N, which is much larger than the sedimentation force on a bead (about 3.5×10^{-15} N) calculated according to the density difference between beads and water. To make the beads settle down onto the electrodes, the applied voltage must be less than ~ 0.67 V_{pp} and the flow rate must be extremely low, which are not the conditions in desired applications of this device as a filter. Here it becomes obvious that the vertical DEP force levitates the beads all the way to the top of the chamber and the horizontal DEP force directs the beads only to the places right above the centers of the electrodes (if no fluidic drag force exists). If we vary the flow rate and measure the corresponding minimum voltages to capture the beads, we obtain the holding characteristic of the trap for a particular set of experimental conditions. From (3) and (4) it is known that the DEP force is related to the square of the voltage and from (6) the hydrodynamic drag force is proportional to the flow rate. Thus, a straight line is expected if we plot the square of the applied capturing voltage versus the flow rate. The result for 2.4 μm beads is shown in Fig. 5, and as expected, a linear relationship between the square of the capturing voltages and the flow rates can be seen. The parameters used for the curve fitting are the frequency (1 MHz), the dielectric constants and conductivities of the beads and the medium, the dynamic viscosity of the medium, and the geometry of the chamber cross section. It is noted that there is no free parameter in this case. The data points are each shown in the form of an average with error bar. The errors could come from the variations of the particle size and their dielectric properties, vibration and unevenness of the fluidic flow and field imperfection on the electrode array. The above experiment was repeated for 5.4 μm beads and a linear relationship was also obtained as shown in Fig. 5, but a decrease in the capturing voltage is seen

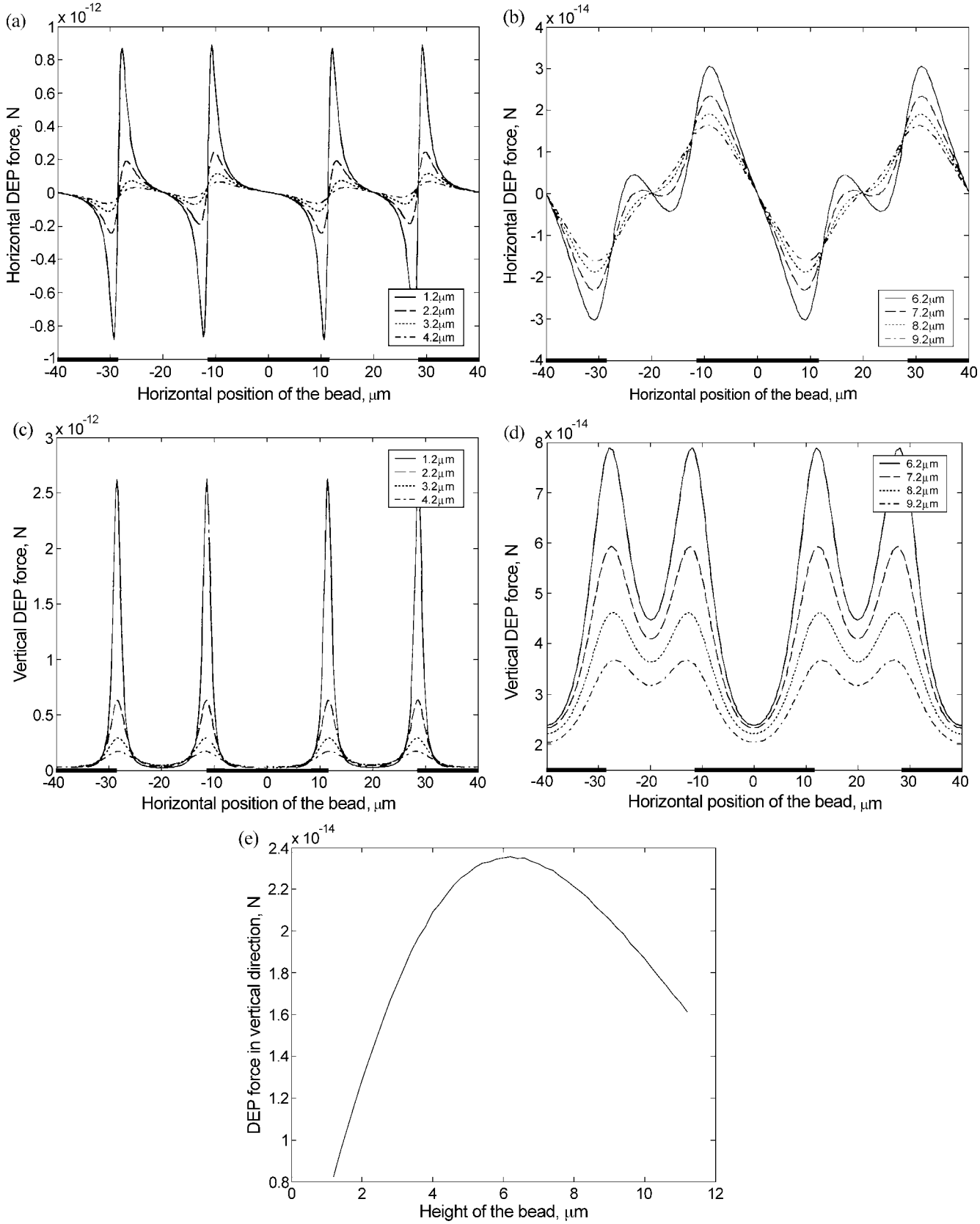

Fig. 4. Horizontal DEP force changes for a 2.4-μm-diameter bead with height from 1.2 μm to 4.2 μm in (a) by taking the conductivity of the beads to be 2×10^{-4} S/m, at 1 V_{pp} and 1 MHz, and from 6.2 μm to 9.2 μm in (b) which showing the beads are directed only to the electrode centers at height above 8 μm. The vertical DEP forces at different heights are shown in (c) and (d) at corresponding heights. (e) shows the minimum vertical force above the center of the electrode changing with height.

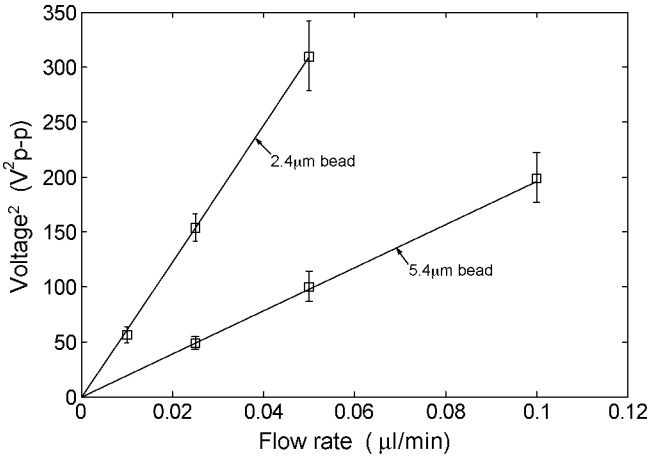

Fig. 5. Linear relationship between the square of the release voltages and the flow rate for 2.4 μm beads and 5.4 μm beads. The frequency was 1 MHz and the conductivity of the suspending medium was 2.5×10^{-4} S/m.

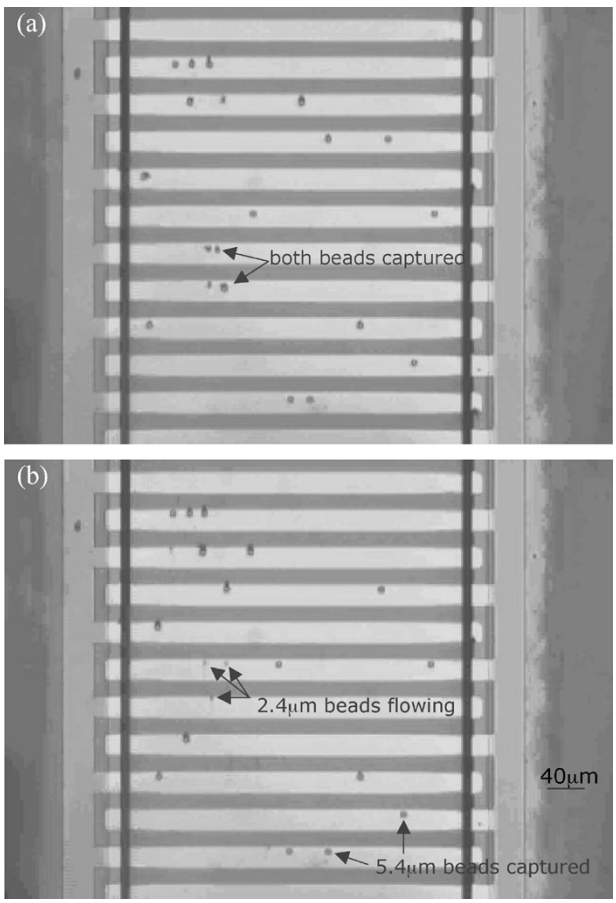

Fig. 6. Both 2.4 and 5.4 μm beads were captured in (a) at about 0.05 μl/min and 20 V_{pp}. The 2.4 μm beads were released when the voltage was decreased to $\sim$ 14 V_{pp} in (b).

compared to the 2.4 μm beads at the same flow rate. This can be used to separate beads with different sizes as we demonstrated in Fig. 6(a) and (b), which are framed out from a video. The match between the experiment with beads and the calculation is significant, thus we validate our ability to model this dielectrophoretic filter by our simulation.

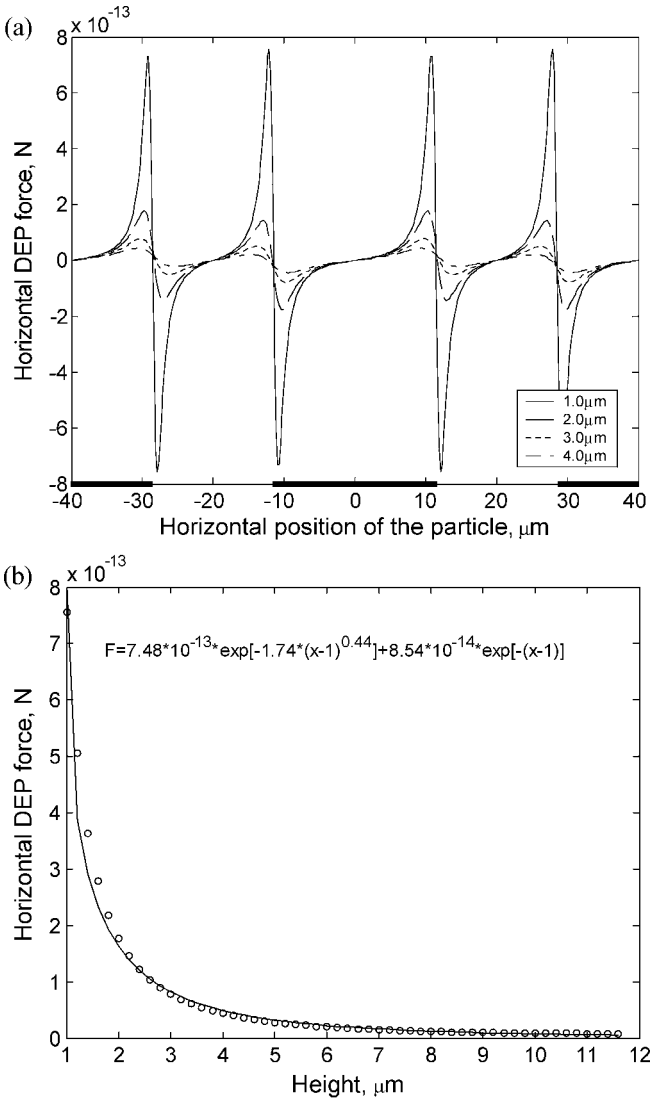

Fig. 7. Horizontal DEP forces for a virtual particle with diameter of 2 μm and polarization factor of 0.5 at 1 MHz and 1 V_{pp} at different heights in (a). The DEP force change with height is shown in (b).

In the case of real biological particles, the situations are more complicated because of the unknown dielectric constant, conductivity and nonuniform geometry of the particles. For simplicity, the biological particles were considered as homogenous spheres with an equivalent volume and an effective dielectric constant and conductivity at a given frequency in our simulation. If a particle experiences positive DEP at a certain frequency in this dielectrophoretic filter, it will be trapped at the electrode edge if the DEP force is strong enough, as other experimental reports have demonstrated. We calculated the DEP forces for a virtual particle with diameter of $d = 2$ μm and polarization factor of 0.5 at 1 MHz and 1 V_{pp}. The horizontal DEP forces at different heights are shown in Fig. 7(a) (the vertical DEP force is quite similar to those in Fig. 4(c) and (d) except that the direction of the force is the opposite). It is seen that the force maxima locate very close to the electrode edge and direct the particles to the edge from both sides. The DEP force decreases very rapidly with height as seen in Fig. 7(b). Huang *et al.* [24] and H. Morgan *et al.* [16] developed analytical expressions for

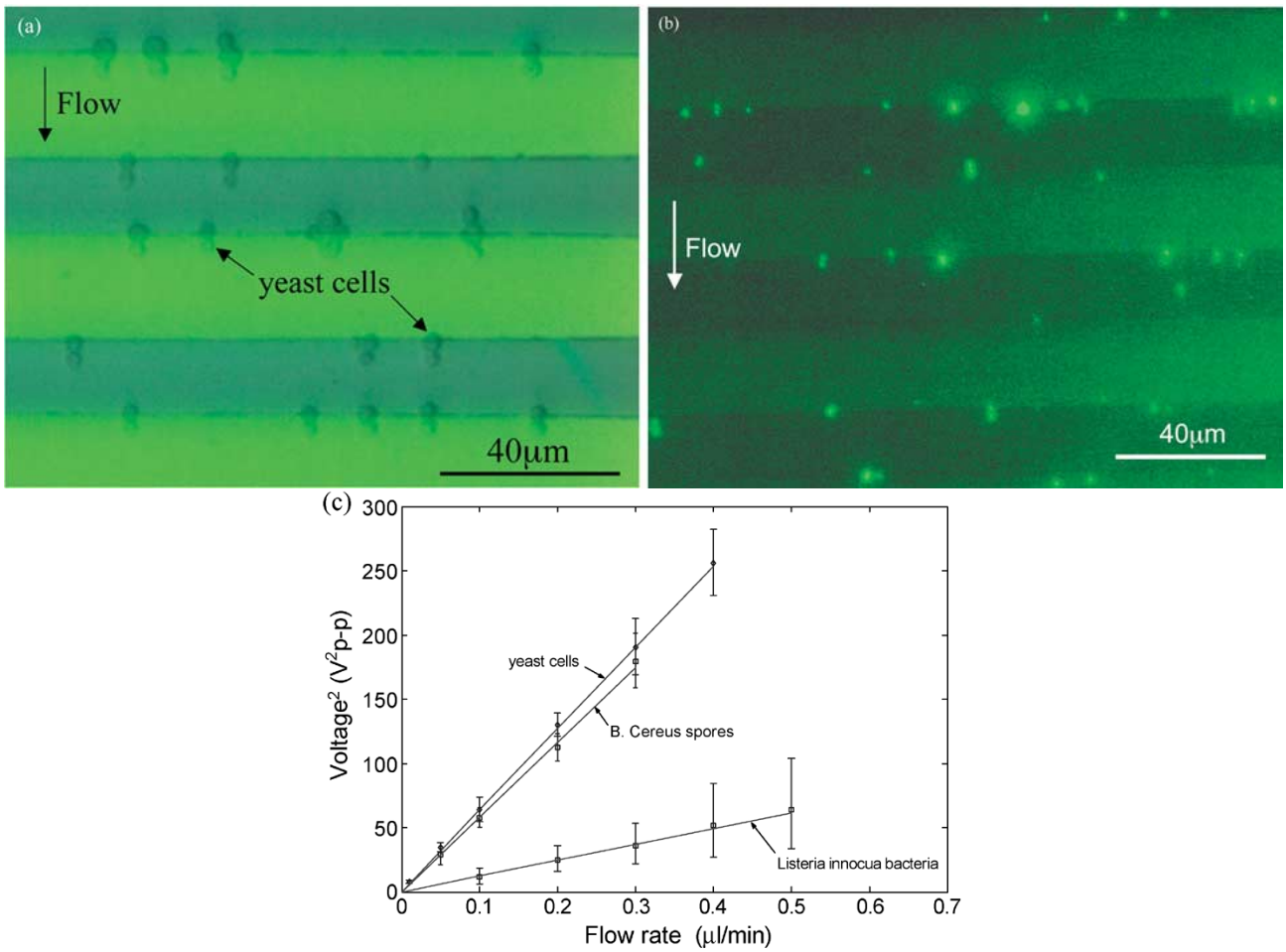

Fig. 8. (a) and (b) show the yeast cells and spores were captured at the electrode edges against the flow at 1 MHz, 20 V_{pp} and $\sim 0.2\ \mu l/min$, respectively. The capturing voltages versus flow rate for yeast, spores and bacteria are shown in Fig. 8(c). Lines were not obtained by least-square fitting but calculated by choosing the appropriate effective conductivity only. Linear relationships were also found between the capturing voltage square and the flow rate.

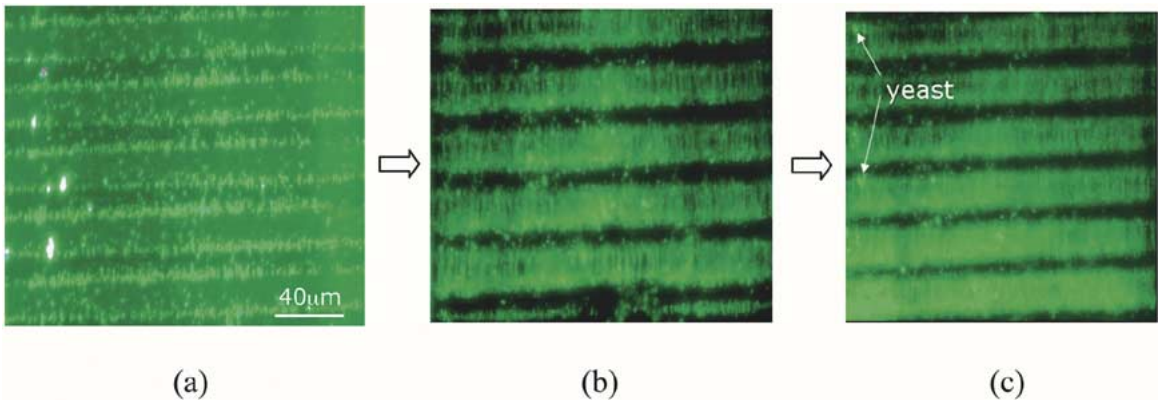

Fig. 9. Time accumulation of *Listeria innocua* bacteria, while yeast cells are flushed away (sample concentrations about $10^{6\sim7}/ml$, at 18 V_{pp}, 1 MHz and flow rate $\sim$ 1 $\mu l/min$, time interval $\sim$5 min, very few yeast cells captured). The small dots (and the accumulation) are the bacteria.

the force, at heights greater than electrode width, to be proportional to $e^{(-\pi h/w)}/w^3$, where h is the height and w is the electrode width. This can't be applied to the case where the particle is close to the electrode plane. Our least square fitting to the calculated forces indicates that when the height is greater than $\sim 1.5d$ ($3\ \mu m$), the force decreases exponentially (e^{-h}) with the height, while the force decreases much faster (with a decaying factor of $\sim e^{-1.74h^{0.44}}$) when the particle is very close to the electrode with height less than $1.5d$.

In the following experiments, biological entities were each suspended in DI water with the same conductivity and voltages were applied to the electrodes of frequency 1 MHz, at which all these particles experienced positive DEP and were collected at the electrode edges. The maximum electric field in the ex-

periments was about 10^4 V/cm, which is believed to be not detrimental to the yeast cells and bacteria [25]. Fig. 8(a) and (b) show that the yeast cells and spores were captured at the electrode edges against the flow respectively. We also measured the capturing voltage versus flow rate for each type of particles, as shown in Fig. 8(c), in which lines were calculated by adjusting the effective conductivities only. Linear relationships were also found between the capturing voltage square and the flow rate, which are consistent with previous studies [10]. The *Saccharomyces cerevisiae* yeast cells, *Bacillus cereus* spores, *Listeria innocua* bacteria were simulated with the average diameter of 5, 1, and 0.8 μm (here bacteria were considered to be equivalent spheres with the same volume of their ellipsoidal shape) and polarization factor of 0.16, 0.11, and 0.48, respectively. The used dielectric constants of yeast cells, spores and bacteria were obtained by setting the dielectric constant to be 50 according to the literatures [3], [23] (while data for *Listeria* bacteria is not available yet) and the conductivities to be 6.8×10^{-3} S/m, 5.9×10^{-3} S/m and 1.3×10^{-2} S/m, respectively. It can be seen that the variations of the data for the biological species are larger than those of the polystyrene beads, which may be due to their large variation in sizes and dielectric properties. It is also seen that there is a large difference between the capturing voltages for *Listeria* bacteria and yeast cells or spores at a given flow rate. Fig. 9 shows that using this DEP filter, a mixture with concentration as high as $\sim 10^7$/ml of *Listeria* bacteria and yeast cells were seen to be separated with good efficiency by capturing and accumulating the *Listeria* bacteria at the electrode edges while letting the yeast cells flowing through the chamber.

It should be noted that by definition, release voltage is the minimum voltage needed for a particle to stay at its equilibrium position at a given flow rate by only considering the force equilibrium. Thus it is different from the "stopping" voltage when considering trapping a particle entering the chamber with initial velocity and height. This will be addressed in the follow-up study.

V. Conclusion

In this study, a microfabricated dielectrophoretic filter with a thin chamber and interdigitated electrode array as a test bed for dielectrophoretic trapping of polystyrene beads and biological entities such as yeast cells, spores and bacteria. Experimental results and computer finite element modeling on the holding forces for both positive and negative dielectrophoretic traps on the microfabricated interdigitated electrodes were presented. First, polystyrene beads were used as a model system and the voltages necessary to capture beads with different diameters against destabilizing fluid flows at a given frequency were measured. The experimental results and those from modeling are found to be in close agreement, with no adjusted parameters, validating our ability to model the dielectrophoretic filter. Then, different biological species were used and the capturing characteristic of the DEP filter for particles experiencing positive DEP were found to be quite close to what the model predicted. The combination of experiments and modeling has given insight into the DEP forces over the interdigitated electrodes and can be very useful in designing and operating a dielectrophoretic barrier or filter to sort and select particles entering the microfluidic devices for further analysis.

Acknowledgment

The authors thank Prof. A. Bhunia, Prof. M. Ladisch, and R. Gomez for valuable discussions, and Prof. A. I. Aronson and Dr. T. Walter of Department of Biological Sciences at Purdue University for supplying the spore sample.

References

[1] H. A. Pohl, *Dielectrophoresis*. Cambridge, U.K.: Cambridge University Press, 1978.

[2] G. H. Markx, M. S. Talary, and R. Pethig, "Separation of viable and nonviable yeast using dielectrophoresis," *J. Biotechnol.*, vol. 32, pp. 29–37, 1994.

[3] Y. Huang, R. Holzel, R. Pethig, and X. B. Wang, "Differences in the AC electrodynamics of viable and nonviable yeast cells determined through combined dielectrophoresis and electrorotation studies," *Phys. Med. Biol.*, vol. 37, no. 7, pp. 1499–1517, 1992.

[4] H. Li and R. Bashir, "Dielectrophoretic separation and manipulation of live and heat-treated cells of listeria on microfabricated devices with interdigitated electrodes," *Sens. Actuators B, Chem.*, vol. 86, pp. 215–221, 2002.

[5] X. B. Wang, Y. Huang, P. R. C. Gascoyne, and F. F. Becker, "Dielectrophoretic manipulation of particles," *IEEE Trans. Ind. Appl.*, vol. 33, no. 3, pp. 660–669, 1997.

[6] M. P. Hughes, "Strategies for dielectrophoretic separation in laboratory-on-a-chip systems," *Electrophoresis*, vol. 23, pp. 2569–2582, 2002.

[7] X. B. Wang, J. Vykoukal, F. F. Becker, and P. R. C. Gascoyne, "Separation of polystyrene microbeads using dielectrophoretic/gravitational field-flow-fractionation," *Biophys. J.*, vol. 74, pp. 2689–2701, 1998.

[8] J. Yang, Y. Huang, X. B. Wang, F. F. Becker, and P. R. C. Gascoyne, "Cell separation on microfabricated electrodes using dielectrophoretic/gravitational field-flow fractionation," *Anal. Chem.*, vol. 71, no. 5, pp. 911–918, 1999.

[9] X. B. Wang, J. Yang, Y. Huang, J. Vykoukal, F. F. Becker, and P. R. C. Gascoyne, "Cell separation by dielectrophoretic field-flow-fractionation," *Anal. Chem.*, vol. 72, no. 4, pp. 832–839, 2000.

[10] G. H. Markx and R. Pethig, "Dielectrophoretic separation of cells: continuous separation," *Biotechnol. Bioeng.*, vol. 45, pp. 337–343, 1995.

[11] M. Washizu and T. B. Jones, "Multipolar dielectrophoretic force calculation," *J. Electrostat.*, vol. 33, pp. 187–198, 1994.

[12] T. B. Jones and M. Washizu, "Multipolar dielectrophoretic and electrorotation theory," *J. Electrostat.*, vol. 37, pp. 121–134, 1996.

[13] P. V. Gerwen, W. Laureyn, W. Laureys, G. Huyberechts, M. O. D. Beeck, K. Baert, J. Suls, W. Sansen, P. Jacobs, L. Hermans, and R. Mertens, "Nanoscaled interdigitated electrode arrays for biochemical sensors," *Sens. Actuators B, Chem.*, vol. 49, pp. 73–80, 1998.

[14] X. J. Wang, X. B. Wang, F. F. Becker, and P. R. C. Gascoyne, "A theoretical method of electrical field analysis for dielectrophoretic electrode arrays using green's theorem," *J. Phys. D: Appl. Phys.*, vol. 29, pp. 1649–1660, 1996.

[15] D. S. Clague and E. K. Wheeler, "Dielectrophoretic manipulation of macromolecules: the electric field," *Phys. Rev. E*, vol. 64, pp. 026 605-1–026 605-8, 2001.

[16] H. Morgan, A. G. Izquierdo, D. Bakewell, N. G. Green, and A. Ramos, "The dielectrophoretic and travelling wave forces generated by interdigitated electrode arrays: analytical solution using fourier series," *J. Phys. D: Appl. Phys.*, vol. 34, pp. 1553–1561, 2001.

[17] N. G. Green, A. Romas, and H. Morgan, "Numerical solution of the dielectrophoretic and travelling wave forces for interdigitated electrode arrays using the finite element method," *J. Electrostat.*, vol. 56, pp. 235–254, 2002.

[18] J. Voldman, M. Toner, M. L. Gray, and M. A. Schmidt, "Design and analysis of extruded quadrupolar dielectrophoretic traps," *J. Electrostat.*, vol. 57, pp. 69–90, 2003.

[19] J. Voldman, R. A. Braff, M. Toner, M. L. Gray, and M. A. Schimidt, "Holding forces of single-particle dielectrophoretic traps," *Biophys. J.*, vol. 80, no. 1, pp. 531–541, 2001.

[20] A. J. Goldman, R. G. Cox, and H. Brenner, "Slow viscous motion of a sphere parallel to a plane wall—II Couette flow," *Chem. Eng. Sci.*, vol. 22, pp. 653–660, 1967.
[21] P. S. Williams, T. Koch, and J. C. Giddings, "Characterization of near-wall hydrodynamic lift forces using sedimentation field-flow fractionation," *Chem. Eng. Commun.*, vol. 111, pp. 121–147, 1992.
[22] R. Gomez, R. Bashir, A. Sarikaya, M. Ladisch, J. Sturgis, J. Robinson, T. Geng, A. Bhunia, H. Apple, and S. Wereley, "Microfluidic biochip for impedance spectroscopy of biological species," *Biomed. Microdev.*, vol. 3, no. 3, pp. 201–209, 2001.
[23] E. L. Carstensen, R. E. Marquis, and P. Gerhardt, "Dielectric study of the physical state of electrolytes and water within Bacillus cereus spores," *J. Bacteriol.*, vol. 107, pp. 106–113, 1971.
[24] Y. Huang, X. B. Wang, F. F. Becker, and P. R. C. Gascoyne, "Introducing dielectrophoretesis as a new force field for field-flow-fractionation," *Biophys. J.*, vol. 73, pp. 1118–1129, 1997.
[25] S.-W. Lee and Y.-C. Tai, "A micro cell lysis device," *Sens. Actuators A, Phys.*, vol. 73, no. 1–2, pp. 74–79, 1999.

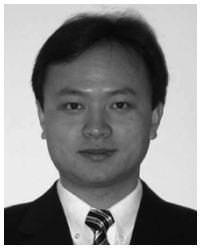

Haibo Li received the B.S. and M.S. degrees in materials science and engineering from Tsinghua University, Beijing, China, in 1996 and 1999, respectively.

He is currently working towards the Ph.D. degree and is a Research Assistant in the School of Electrical and Computer Engineering at Purdue University, West Lafayette, IN. He works in the BioMEMS group with Dr. R. Bashir on design, fabrication and characterization of dielectrophoretic devices, dielectrophoresis theory, simulation and its applications in biochips.

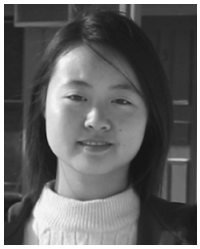

Yanan Zheng received the B.S. degree in biomedical engineering from Southeast University, Nanjing, China, in 2001.

She is currently working towards the Ph.D. degree and is a Research Assistant in the Department of Biomedical Engineering, Purdue University, West Lafayette, IN. She works with Dr. A. Rundell on the mathematical modeling of multivalent antigen capture by immunosurfaces and the T-cell antigen-activated signal transduction pathways from both experimental and modeling aspects.

Demir Akin received the D.V.M. degree from Ankara University, Turkey, in 1988, the M.S. degree in microbiology from Mississippi State University in 1991, and the Ph.D. degree in molecular virology from Purdue University, West Lafayette, IN, in 1998.

He did his postdoctoral work in the areas of molecular biology and viral bioinformatics at the Indiana State Animal Disease Diagnostic Laboratory from 1998 to 2000. He became a Research Scientist in the School of Nuclear Engineering at Purdue University in 2001 and worked on artificial intelligence-based In-Silico Biology and Genomics software development. As a research scientist, he joined the Electrical and Computer Engineering Department at Purdue University in 2002 and became a Senior Research Scientist in 2003. His current research projects and interests include integration of biology in engineering, nanomedicine, BioMEMS-based sensors and devices with medical diagnostic and therapeutic potential, single molecule imaging using fluorescence microscopy and atomic force microscopy, systems biology, and pathogenic and biodefense-related infectious agent diagnostics.

Rashid Bashir (S'90–M'92–SM'01) received the B.S.E.E. degree from Texas Tech University, Lubbock, as the highest-ranking graduate in the College of Engineering in December 1987. He creceived the M.S.E.E. and Ph.D. degrees from Purdue University, West Lafayette, IN, in 1989 and 1992, respectively.

From October 1992 to October 1998, he worked at National Semiconductor in the Process Technology Development Group as a Senior Engineering Manager. His group worked on developing state-of-the-art bipolar and BiCMOS process for high voltage, analog and RF applications, SiGe HBT devices, SOI-bonded wafers, and MEMS technologies. He is currently an Associate Professor of Electrical and Computer Engineering at Purdue University since October 1998 and Associate Professor of Biomedical Engineering at Purdue University since June 2000. He has authored or coauthored over 100 journal and conference papers and over 25 patents. His research interests include MEMS, BioMEMS, applications of semiconductor fabrication to biomedical engineering, advanced semiconductor fabrication techniques, and nanobiotechnology.

Dr. Bashir received the NSF Career Award for his work in Biosensors and BioMEMS in 2000. He also received the Joel and Spira Outstanding Teaching award from School of ECE at Purdue University, and the Technology Translation Award from the 2001 BioMEMS and Nanobiotechnology World Congress Meeting, Columbus, OH. He was also selected by National Academy of Engineering to attend the Frontiers in Engineering Workshop in Fall 2003.